Periodic orbit quantization of the closed three-disk billiard as an example of a chaotic system with strong pruning

Kirsten Weibert, Jörg Main, and Günter Wunner
Institut für Theoretische Physik 1, Universität Stuttgart, D-70550 Stuttgart, Germany
(Dated: February 8, 2008)

Classical chaotic systems with symbolic dynamics but strong pruning present a particular challenge for the application of semiclassical quantization methods. In the present study we show that the technique of periodic orbit quantization by harmonic inversion of trace formulae, which does not rely on the existence of a complete symbolic dynamics or other specific properties, lends itself ideally to calculating semiclassical eigenvalues from periodic orbit data even in strongly pruned systems. As the number of periodic orbits proliferates exponentially in chaotic systems, we apply the harmonic inversion technique to cross-correlated periodic orbit sums, which allows us to reduce the required number of orbits. The power of the method is demonstrated for the closed three-disk billiard as a prime example of a classically chaotic bound system with strong pruning.

PACS numbers: 05.45.−a, 03.65.Sq

I. INTRODUCTION

The relation between quantum spectra, on the one hand, and the dynamics of the corresponding classical systems, on the other, is a problem of fundamental importance in physics, which has attracted attention ever since the early days of quantum mechanics. A key to understanding this relation in chaotic systems was Gutzwiller's discovery (cf. [1, 2]) that the semiclassical density of states in these systems can be written as a sum over all (isolated) periodic orbits of the classical system. However, practical applications of Gutzwiller's trace formula, like other periodic orbit sums, are greatly impeded by the fact that the sums usually diverge in the domain where the physical eigenvalues are located, mainly as a consequence of the rapid proliferation of periodic orbits with growing period. Various techniques were developed over the years to overcome the convergence problem of the periodic orbit sums [3, 4, 5], but most of them depend on special properties of the systems, such as ergodicity or the existence of complete symbolic dynamics.

As an alternative, the technique of harmonic inversion of semiclassical trace formulae has been introduced as a very general method for extracting eigenvalues from periodic orbit sums for both chaotic and regular systems [6, 7, 8, 9, 10, 11]. Harmonic inversion circumvents the convergence problems, and allows one to obtain the semiclassical eigenvalues from a relatively small number of periodic orbits. Moreover, the method does not require any special properties of the systems, and therefore is applicable also to the particularly challenging case of systems with strong pruning, i.e., systems with a highly incomplete symbolic coding of the periodic orbits. In this paper we demonstrate the power of the harmonic inversion technique in the semiclassical quantization of the closed three-disk billiard system, for which all other semiclassical quantization methods to date have failed in determining more than the few lowest eigenvalues, chiefly because of the extremely rapid proliferation of periodic orbits with increasing action and the strong pruning typical of this system. From a technical point of view our study will show that harmonic inversion is numerically stable even when handling huge (on the order of several million) periodic orbit sets.

The three-disk billiard system consists of three equally spaced hard disks of unit radius. The existence or nonexistence of periodic orbits and the behavior of the periodic orbit parameters in the three-disk system sensitively depend on the distance d between the centers of the disks. Large disk separations, especially $d = 6$, have served as a test case for periodic orbit quantization of chaotic systems in many investigations in recent years. In particular, the system has been employed as prototype example for the usefulness of periodic orbit quantization by cycle expansion techniques [3, 12, 13, 14]. For large disk separations, the assumptions of the cycle expansion, namely that the contributions from long orbits are shadowed by those of short orbits, are almost exactly fulfilled. This is no longer true for small disk separations. As the disks approach each other, the convergence of the cycle expansion becomes slower and slower, until it finally breaks down.

Periodic orbit quantization by harmonic inversion does not depend on specific properties, such as shadowing of orbits etc., and therefore is expected to work well also for small disk separations. In fact, the harmonic inversion technique has successfully been applied to the "standard" literature disk separation $d = 6$ as well as to the small distance $d = 2.5$, where the convergence of the cycle expansion is already slow [7, 8]. In this paper we concentrate on the limiting case of mutually touching disks, $d = 2$, where the system turns into a bound system, and the requirements of the cycle expansion and other semiclassical methods are no longer fulfilled at all.

For the closed three-disk system, the lowest exact quantum eigenvalues were first calculated by Tanner et al. [15] and by Scherer [16]. A remarkable step towards the semiclassical quantization of the closed three-disk system was achieved by combining the conventional cycle expansion with a functional equation [15]. Based on

periodic orbit corrections to the mean density of states, approximations to the very lowest eigenvalues could be obtained from a small set of periodic orbits up to cycle length $l = 3$, where the symbolic dynamics is still complete (including formally a zero length orbit). For the very lowest eigenvalues, the results were found to be in good agreement with the exact quantum values. However, the method failed for higher eigenvalues, where only the mean density of states could be reproduced. Since the problems with the method arose from the strong pruning of orbits in this system, they are of a fundamental nature, and could not be overcome by including more orbits. No other semiclassical method has been successful in obtaining higher eigenvalues in the closed three-disk billiard system yet. In this paper, we will demonstrate that harmonic inversion passes even this acid test of semiclassical quantization.

In Sec. II we discuss the construction of the periodic orbit signal for the closed three-disk system, which is a nontrivial task because of, firstly, the extremely rapid proliferation of periodic orbits and, secondly, the strong pruning of the symbolic dynamics. Once the signal has been constructed, we refer in Sec. III to the harmonic inversion technique for the extraction of the semiclassical eigenvalues. The numerical recipe of the harmonic inversion method has already been established in the literature [6, 7, 8, 9, 10, 11], however, to make the article self-consistent we recapitulate the important steps in Sec. III A. The semiclassical results are discussed in Secs. III B and III C.

II. PERIODIC ORBITS OF THE CLOSED THREE-DISK SYSTEM

We start by summarizing the basic properties of the three-disk system relevant for periodic orbit quantization. Furthermore, the pruning of orbits and the distribution of the orbit parameters are investigated, and the resulting strategies for the numerical search for periodic orbits are discussed.

A. Symbolic code and symmetry reduction

The periodic orbits of the three-disk system can be labeled by a ternary symbolic code, which is complete for sufficiently large disk separations. The classical dynamics of the three-disk system has been studied, among others, by Gaspard and Rice [17]. If the disks are labeled by the numbers 1, 2, 3, each periodic orbit is characterized by a sequence of these numbers, indicating the disks the particle collides with during one period of the orbit. For sufficiently separated disks, there is a one-to-one correspondence between the symbolic code and the periodic orbits of the system: For every sequence there exists one unique periodic orbit (with the restriction that consecutive repetitions of the same symbol are forbidden

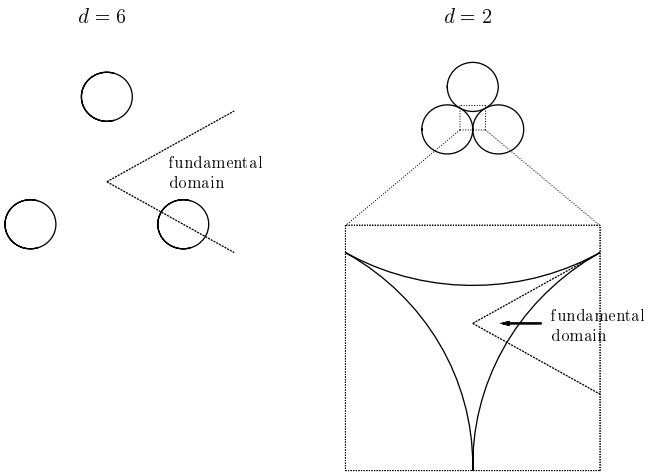

FIG. 1: Open and closed three-disk system. The fundamental domain consists of a one-sixth slice of the full system.

and circular shifts of a sequence describe the same orbit). As was first pointed out by Hansen [18], at disk separation $d = 2.04821419$ "pruning" sets in, i.e., part of the periodic orbits become unphysical as they begin to run through one of the disks, and thus the symbolic code is no longer complete. The number of pruned orbits rapidly becomes larger and larger if the disks continue to approach each other. In the limiting case of touching disks, $d = 2$, the system exhibits strong pruning. Examples of pruned orbits will be discussed in Section II C.

In our calculations, we make use of the symmetry reduction introduced by Cvitanović and Eckhardt in Ref. [3]: The three-disk system is invariant under the symmetry operations of the group C_{3v}, i.e., reflections at three symmetry lines and rotations by $2\pi/3$ and $4\pi/3$. The periodic orbits fall into three classes of distinct symmetry: orbits invariant under reflections at one of the symmetry lines (multiplicity 3), orbits invariant under rotations by $2\pi/3$ and $4\pi/3$ (multiplicity 2), and orbits with no symmetry (multiplicity 6). The quantum states are grouped in the three irreducible subspaces A_1, A_2, and E, where the states of the A_1 (A_2) subspace are symmetric (antisymmetric) under reflection at the symmetry lines, respectively, and the states of the E subspace are invariant under rotations by $2\pi/3$ and $4\pi/3$.

Following Refs. [3, 13], one can map the system onto a fundamental domain, which consists of a one-sixth slice of the full system, with the symmetry axes acting as straight mirror walls (see Fig. 1). The periodic orbits of the full system can be described completely in terms of the periodic orbits in the fundamental domain. The symmetry reduced periodic orbits are labeled by a binary code, where the symbol '0' represents backscattering (or change between clockwise and anti-clockwise scattering) and the symbol '1' stands for scattering to the third disk in the original full domain picture. For example, the

shortest full domain orbit 12 maps onto the 0 orbit, and the 123 orbit maps onto the 1 orbit.

B. Semiclassical density of states

The quantum resonances of the three different subspaces A_1, A_2 and E can be obtained separately from the periodic orbits in the fundamental domain by introducing appropriate weight factors for the orbits in Gutzwiller's trace formula, as was shown by Cvitanović and Eckhardt [19]. We concentrate on the A_1 subspace, for which each orbit has a weight factor equal to 1.

As for all billiard systems, the shape of the periodic orbits is independent of the wave number $k = \sqrt{2mE}/\hbar$, and the action scales as

$$S/\hbar = ks, \tag{1}$$

where the scaled action s is equal to the physical length of the orbit. We consider the density of states as a function of the wave number

$$\rho(k) = -\frac{1}{\pi}\,\mathrm{Im}\; g(k)\;, \tag{2}$$

with a scaled response function $g(k)$. Applying the Gutzwiller trace formula to the closed three-disk system yields for the A_1 subspace

$$\begin{aligned} g(k) &= g_0(k) - \mathrm{i}\sum_{\mathrm{po}} \frac{s_{\mathrm{po}}\,\mathrm{e}^{-\mathrm{i}\frac{\pi}{2}\mu_{\mathrm{po}}}}{r|\det(M_{\mathrm{po}}-1)|^{1/2}}\;\mathrm{e}^{\mathrm{i}ks_{\mathrm{po}}} \qquad (3)\\ &= g_0(k) - \mathrm{i}\sum_{\mathrm{po}}(-1)^{l_s}\frac{s_{\mathrm{po}}}{r|(\lambda_{\mathrm{po}}-1)(\frac{1}{\lambda_{\mathrm{po}}}-1)|^{1/2}}\;\mathrm{e}^{\mathrm{i}ks_{\mathrm{po}}}\,, \end{aligned}$$

where M_{po} and μ_{po} are the monodromy matrix and the Maslov index of the orbit, respectively, l_s is the symbol length, s_{po} is the scaled action, and λ_{po} denotes the expanding stability eigenvalue of the orbit (i.e., the eigenvalue with an absolute value larger than one). The sum runs over all symmetry reduced periodic orbits including multiple traversals. Here, r denotes the repetition number with respect to the corresponding primitive orbit.

In practice, only the primitive periodic orbits have to be determined. The parameters of the r^{th} repetition of the primitive orbit (here characterized by the index 0) are then given by $l_s = rl_{s0}$, $s = rs_0$ and $\lambda = \lambda_0^r$.

C. Numerical search for periodic orbits

For extracting the quantum resonances of the system from Eq. (4) by harmonic inversion, all periodic orbits up to a maximum scaled action have to be included. The parameters of the periodic orbits – scaled action and stability eigenvalues – have to be determined numerically. We calculate the primitive periodic orbits using the symbolic code as input. For simplicity, the calculations are carried out in the full domain, and the results are then translated back into the symmetry reduced system. The disks are "connected" according to the code, starting with arbitrary reflection points on the disks as initial condition. The reflection points are then varied in such a way that the total length (i.e., the action) of the orbit reaches a minimum. All orbit parameters can then be calculated from the reflection points. The scaled action is given by the length of the (symmetry reduced) orbit, and the stability eigenvalue λ can be determined by an algorithm proposed by Bogomolny [20]. In addition to action and stability, one can also determine averages of different classical quantities (distance from the center of the system, angular momentum, etc.), which are needed for the cross-correlation technique (see Section III).

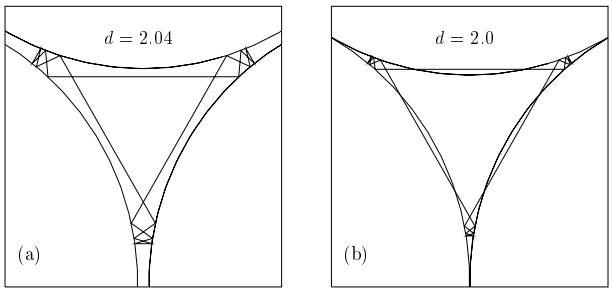

FIG. 2: An example of the first class of pruned orbits (see text), plotted in full domain representation. The symmetry reduced code of the orbit is 000011. The orbit is shown at two different disk separations d, indicated at the top of each diagram. At $d = 2.04$, the orbit is still physical, at $d = 2.0$ it has become unphysical as is penetrates the disks.

For disk separations smaller than the pruning limit $d = 2.04821419$, it has to be checked whether or not the orbits are physical, i.e., whether or not they stay completely outside the disks. In our numerical calculations, we found two different classes of pruned orbits. An example of the first class is given in Figure 2: As the disks approach each other, a section of the orbit connecting two of the disks gets inside the third disk. The pruned orbit still corresponds to a unique minimum of the total length when the reflection points on the disks are varied for given symbolic code. This is not the case for the second class, an example of which is shown in Figure 3: In this case, as the disks come closer, the reflection angle at one specific reflection point approaches π. As the value π is reached, the minimum of the action with respect to this specific reflection point splits into two equal minima and one local maximum. Accordingly, the orbit splits into three unphysical orbits with the same symbolic code.

In one case, the orbit is now reflected on the inside of the disk (see Fig. 3c), which corresponds to a reflection angle larger than π (i.e., the orbit has penetrated into the disk in the vicinity of the reflection point). This orbit does not correspond to a minimum of the total length but to a saddle point. In the other two cases, Figs. 3d and 3e, the reflection point moves along the disk in such

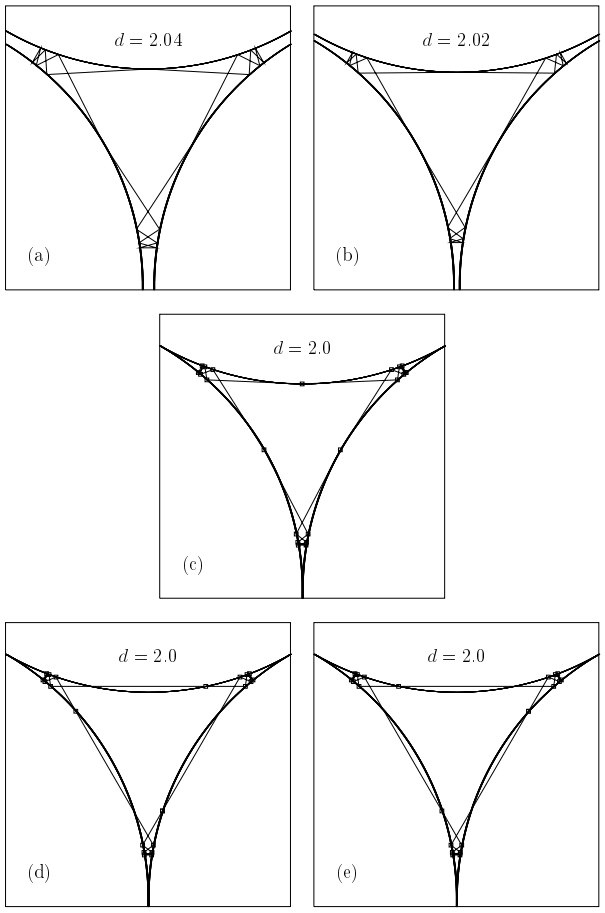

FIG. 3: An example of the second class of pruned orbits (see text), plotted in full domain representation. The symmetry reduced code of the orbit is 0000001. The orbit is still physical at disk separations $d = 2.04$ and $d = 2.02$. At $d = 2.0$ it has split into three unphysical orbits. The squares indicate the "reflection points". Note in (c) that the reflection angle at the three central reflection points is larger than π, i.e., the orbit in fact penetrates into the disks in the vicinity of these points.

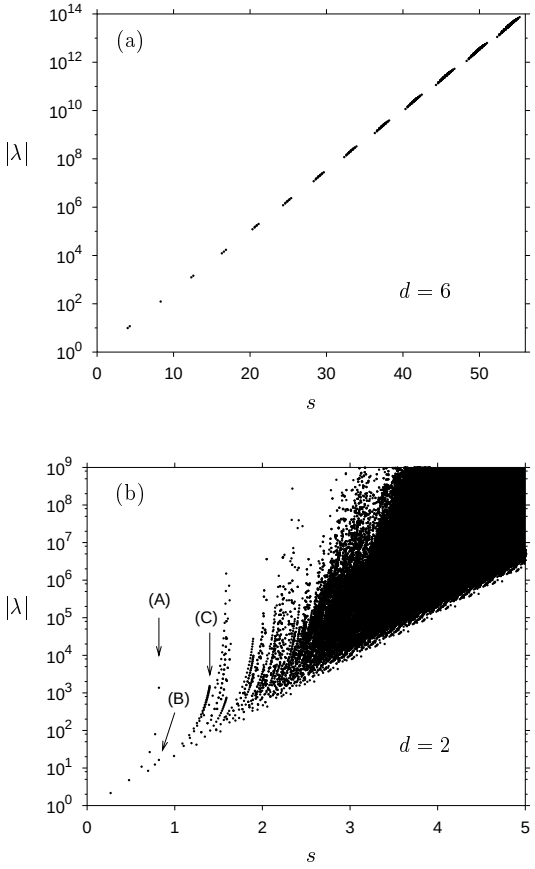

FIG. 4: Distribution of periodic orbit parameters of the three-disk system (a) with disk separation $d = 6$, and (b) in the case of touching disks, $d = 2$. The quantities plotted are the absolute value of the larger stability eigenvalue $|\lambda|$ versus the physical length s of the orbits. For $d = 2$, for clarity a few channels of orbits are marked by arrows. Channels (A) and (B) break off because of pruning. The two channels marked (C) contain infinitely many orbits, but have been cut off by restricting the maximum number of successive zeros in the symbolic code (see text).

a way that the reflection law is no longer fulfilled but the orbit just passes the "reflection point" in a straight line and penetrates into the disk. These two cases correspond to two equally deep minima of the total length. The two orbits have the same shape but only differ as to which penetration point is considered as "reflection point", indicated by the squares in Figs. 3d and 3e. In fact, the shape of the orbit is equal to that of a pruned orbit with a (symmetry reduced) symbol length that is shorter by 1 and which belongs to the first class of pruned orbits as defined above. (In this orbit the reflection point in question is simply missing, i.e., none of the penetration points is considered as reflection point.)

Besides the existence or nonexistence of periodic orbits, the distance between the disks also strongly influences the distribution of the periodic orbit parameters. This is illustrated in Figure 4, which compares the orbit parameters of the shortest primitive periodic orbits found for the open three-disk system with disk separation $d = 6$ and for the case of touching disks, $d = 2$. For $d = 6$, the action and stability of the orbits are mainly determined by the symbol length, the orbit parameters are nicely bunched in easily distinguishable intervals, and the number of orbits up to a given action is relatively small. However, the picture changes completely when the disks approach each other: As all orbits become shorter, the total number of orbits up to a given action increases rapidly. The parameters of the orbits are no longer simply determined by the symbol length, and their overall behavior becomes much more complicated, as is evident from Figure 4.

For $d = 2$, the orbits can be grouped in "channels" with the same "tail" (end figures) but growing number of lead-

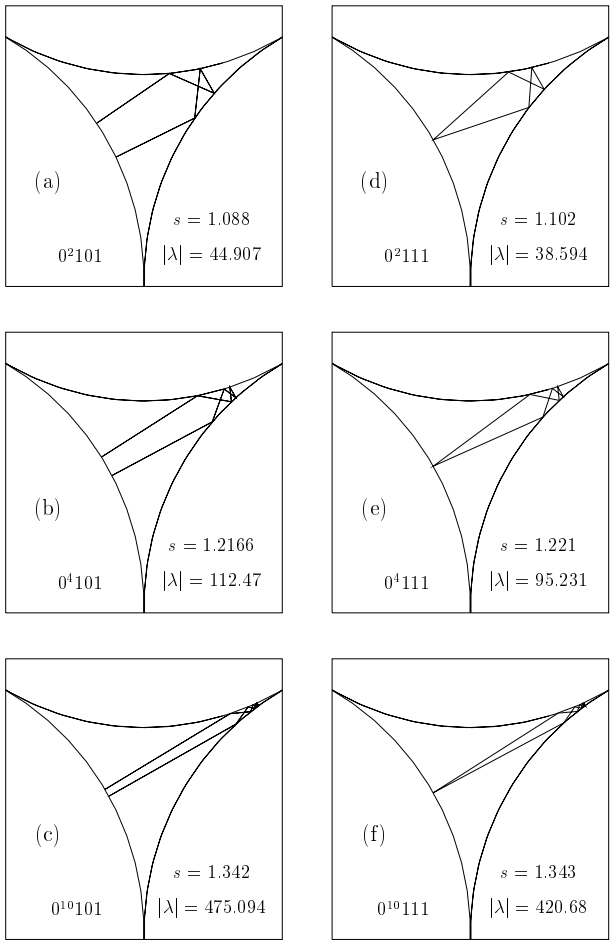

FIG. 5: Examples of orbits of the 0^n101 channel, (a) – (c), and the 0^n111 channel, (d) – (f) (dubbed (C) in Fig. 4b), in full domain representation. With growing number of leading '0's, the orbits run deeper and deeper into the corners between the disks. The series converges towards the limiting orbit that starts exactly in the point where the disks touch and is then directly reflected back from the opposite disk.

ing '0's in the code. (A sequence of n leading '0's in the code will be denoted by 0^n in the following). These orbits have the same basic shape but run deeper and deeper into the corner formed by two touching disks, bouncing back and forth between the two disks (see Fig. 5). In each channel, the action of the orbits grows very slowly with increasing symbol length, while the expanding stability eigenvalue increases relatively fast (in fact exponentially) with every additional collision. Since adding a leading '0' to the symbolic code does not change the action considerably, there is a huge number of orbits with very long symbol lengths but relatively small, and comparable, actions. In fact, most channels break off because of pruning. E.g., the 0^n1 series, labeled (A) in Fig. 4b, breaks off after six orbits, and the 0^n11 series, marked (B), already breaks off after three orbits. Our analysis strongly suggests that there exist only two infinite channels: The 0^n101 and the 0^n111 series, dubbed (C) in Fig. 4b (these channels are only shown up to 20 leading '0's in the code). The shapes and actions of these orbits converge very slowly towards the shape and action of the limiting orbit which starts exactly in the touching point of two disks and is directly reflected back by the opposite disk (cf. Fig. 5). Although all other channels break off because of pruning, the number of orbits in a channel up to a given action often becomes very large (or, in the two cases mentioned, even infinite). Note that the 0 orbit, bouncing back and forth between two disks, does not exist in the closed three-disk system.

While for large disk separations finding all orbits up to a given action simply corresponds to calculating all orbits up to a certain maximum symbol length, the complicated distribution of periodic orbit parameters in the closed three-disk system renders the search for the relevant periodic orbits up to a given action a nontrivial task. Due to the extremely rapid proliferation of periodic orbits with increasing length s, we were not able to determine all orbits up to a given length $s_{\max}$, but we had to introduce restrictions for the orbits to be included. As the amplitude in the Gutzwiller formula depends on the inverse of the stability parameter, a reasonable cutoff criterion is the size of the stability of the orbit. On the other hand, since in each channel the absolute value of the expanding stability eigenvalue grows exponentially fast, the main contributions of each channel to the periodic orbit sum come from the orbits with small symbol lengths. Furthermore, the Maslov indices of adjacent orbits in each channel differ by two, and therefore the periodic orbit amplitudes alternate in sign, which leads to approximate cancellations of terms in the semiclassical trace formula. As a second criterion, we therefore restricted the number of consecutive symbols '0' in the symbolic code, thus selecting the most relevant orbits of each channel.

The orbits were calculated channel by channel, starting from the shortest orbit in the channel and adding more and more leading zeros to the code. The calculation of the channel was broken off if one of the following conditions was fulfilled:

- The action exceeds the maximum action $s_{\max}$.
- The absolute value of the stability eigenvalue exceeds the given value $\lambda_{\max}$.
- The maximum number of consecutive symbols '0' is reached.
- The orbits become pruned.

For the set of periodic orbits shown in Figure 4b, we searched for orbits with physical length $s < s_{\max} = 5.0$. The maximum for the absolute value of the stability eigenvalue was chosen to be $\lambda_{\max} = 10^9$. The maximum number of successive zeros in the code was restricted to 20 for orbits with length $s < 3.1$ and to 12 for orbits with $3.1 < s < 5.0$.

III. PERIODIC ORBIT QUANTIZATION OF THE CLOSED THREE-DISK SYSTEM BY HARMONIC INVERSION

The fundamental problem, and challenge, now is to extract semiclassical eigenvalues in a numerically stable way from the huge periodic orbit set presented in Fig. 4b. To this end, we resort to harmonic inversion of periodic orbit signals [6, 7, 8, 9, 10, 11]. Here, we review the basic ideas and present an extension of the method introduced in [11] to harmonic inversion of cross-correlated periodic orbit sums.

A. The method

The starting point is to introduce a weighted density of states in terms of k

$$\varrho_{\alpha\alpha'}(k) = -\frac{1}{\pi}\,\mathrm{Im}\, g_{\alpha\alpha'}(k)\ , \tag{4}$$

with

$$g^{\mathrm{qm}}_{\alpha\alpha'}(k) = \sum_m \frac{b_{\alpha n} b_{\alpha' n}}{k - k_m + \mathrm{i}\epsilon}\ , \tag{5}$$

where k_m is the eigenvalue of the wave number of eigenstate $|m\rangle$ and

$$b_{\alpha m} = \langle m|\hat{A}_\alpha|m\rangle \tag{6}$$

are the diagonal matrix elements of a chosen set of D linearly independent operators $\hat{A}_\alpha$, $\alpha = 1, 2, \ldots, D$. The Fourier transform of (5) yields a $D \times D$ cross-correlated signal

$$\begin{aligned} C^{\mathrm{qm}}_{\alpha\alpha'}(s) &= \frac{\mathrm{i}}{2\pi}\int_{-\infty}^{+\infty} g_{\alpha\alpha'}(k)\mathrm{e}^{-\mathrm{i}sk}\mathrm{d}k \\ &= \sum_m b_{\alpha m} b_{\alpha' m}\mathrm{e}^{-\mathrm{i}k_m s}\ . \end{aligned} \tag{7}$$

A semiclassical approximation to the weighted quantum response function (5) is given by the semiclassical response function (3) weighted with the classical averages

$$a_{\alpha,\mathrm{po}} = \frac{1}{s_{\mathrm{po}}}\int_0^{s_{\mathrm{po}}} A_\alpha(\mathbf{q}(s),\mathbf{p}(s))\mathrm{d}s\ , \tag{8}$$

with $A_\alpha(\mathbf{q},\mathbf{p})$ the Wigner transform of the operator $\hat{A}_\alpha$ [21, 22]. By Fourier transformation we obtain the semiclassical approximation to the quantum signal (7), which reads

$$\begin{aligned} C^{\mathrm{sc}}_{\alpha\alpha'}(s) &= \sum_{\mathrm{po}} \frac{a_{\alpha,\mathrm{po}}\, a_{\alpha',\mathrm{po}}\, s_{\mathrm{po}}\, \mathrm{e}^{-\mathrm{i}\frac{\pi}{2}\mu_{\mathrm{po}}}}{r|\det(M_{\mathrm{po}} - \mathbf{1})|^{1/2}}\ \delta\left(s - s_{\mathrm{po}}\right) \\ &\equiv \sum_{\mathrm{po}} \mathcal{A}^{\mathrm{po}}_{\alpha\alpha'}\delta\left(s - s_{\mathrm{po}}\right)\ , \end{aligned} \tag{9}$$

where r is the repetition number counting the traversals of the primitive orbit, and M_{po} and μ_{po} are the monodromy matrix and Maslov index of the orbit, respectively. Semiclassical approximations to the eigenvalues k_m, and eventually also to the diagonal matrix elements $\langle m|\hat{A}_\alpha|m\rangle$, are obtained by adjusting the semiclassical cross-correlated periodic orbit signal (9) to the functional form of the quantum signal (7). This can be done with the filter-diagonalization method for the signal processing of cross-correlation functions [23, 24]. Here, we resort to an alternative method introduced in Ref. [11], which will now be extended for the harmonic inversion of cross-correlated periodic orbit sums.

The special form of the periodic orbit signal (9) as a sum of δ functions allows for an even simpler procedure than filter-diagonalization, viz. analytical filtering. In the following we will apply a rectangular filter, i.e., $f(k) = 1$ for frequencies $k \in [k_0 - \Delta k, k_0 + \Delta k]$, and $f(k) = 0$ outside the window. Applying this filter to the semiclassical signal $C^{\mathrm{sc}}_{\alpha\alpha'}(s)$ in (9) we obtain the band-limited (bl) cross-correlated periodic orbit signal,

$$\begin{aligned} C^{\mathrm{sc,bl}}_{\alpha\alpha'}(s) &= \frac{\mathrm{i}}{2\pi}\int_{k_0-\Delta k}^{k_0+\Delta k} g^{\mathrm{sc}}_{\alpha\alpha'}(k)\mathrm{e}^{-\mathrm{i}s(k-k_0)}\mathrm{d}k \\ &= \frac{\mathrm{i}}{2\pi}\sum_{\mathrm{po}}\mathcal{A}^{\mathrm{po}}_{\alpha\alpha'}\int_{k_0-\Delta k}^{k_0+\Delta k}\mathrm{e}^{\mathrm{i}sk_0-\mathrm{i}(s-s_{\mathrm{po}})k}\mathrm{d}k \\ &= \mathrm{i}\sum_{\mathrm{po}}\mathcal{A}^{\mathrm{po}}_{\alpha\alpha'}\frac{\sin\left[(s-s_{\mathrm{po}})\Delta k\right]}{\pi(s-s_{\mathrm{po}})}\mathrm{e}^{\mathrm{i}s_{\mathrm{po}}k_0}\ . \end{aligned} \tag{10}$$

The introduction of k_0 into the arguments of the exponential functions in (10) causes a shift of frequencies by $-k_0$ in the frequency domain. Note that $C^{\mathrm{sc,bl}}_{\alpha\alpha'}(s)$ is a smooth function and can be easily evaluated on an arbitrary grid of points $s_m < s_{\max}$ provided the periodic orbit data are known for the set of orbits with classical action $s_{\mathrm{po}} < s_{\max}$.

Applying now the same filter as used for the semiclassical periodic orbit signal to the quantum one, we obtain the band-limited quantum signal

$$\begin{aligned} C^{\mathrm{qm,bl}}_{\alpha\alpha'}(s) &= \frac{\mathrm{i}}{2\pi}\int_{k_0-\Delta k}^{k_0+\Delta k} g^{\mathrm{qm}}_{\alpha\alpha'}(k)\mathrm{e}^{-\mathrm{i}s(ik-k_0)}\mathrm{d}k \\ &= \sum_{m=1}^{M} b_{\alpha m} b_{\alpha' m}\mathrm{e}^{-\mathrm{i}(k_m-k_0)s}\ ,\ |k_m - k_0| < \Delta k\ . \end{aligned} \tag{11}$$

In contrast to the signal $C^{\mathrm{qm}}_{\alpha\alpha'}(s)$ in Eq. (7), the band-limited quantum signal consists of a *finite* number of frequencies k_m, $m = 1, \ldots, M$, where in practical applications M can be of the order of $\sim$ (50-200) for an appropriately chosen frequency window, Δk. The problem of adjusting the band-limited semiclassical signal in Eq. (10) to its quantum mechanical analogue in Eq. (11) can now be written as a set of nonlinear equations

$$\begin{aligned} C^{\mathrm{sc,bl}}_{\alpha\alpha'}(n\tau) \equiv c_{\alpha\alpha',n} &= \sum_{m=1}^{M} b_{\alpha m} b_{\alpha' m}\mathrm{e}^{-\mathrm{i}k'_m n\tau}\ , \\ n &= 0, 1, \ldots, 2N-1\ , \end{aligned} \tag{12}$$

for the unknown variables, viz. the shifted frequencies, $k'_m \equiv k_m - k_0$, and the parameters $b_{\alpha m}$, $m = 1, \ldots, M$. Note that M is related to the signal length $2N$ and the dimension D of the cross-correlation matrix by $M = ND$. The signal (12) can be evaluated on an equidistant grid, $s = n\tau$, with relatively large step size $\tau \equiv \pi/\Delta w$, and the discrete signal points $c_{\alpha\alpha',n} \equiv C^{\mathrm{sc,bl}}_{\alpha\alpha'}(n\tau)$ are called the "band-limited" cross-correlated periodic orbit signal.

We now wish to solve the nonlinear system, Eq. (12), which can be written as

$$c_{\alpha\alpha',n} = \sum_{m=1}^{M} b_{\alpha m} b_{\alpha' m} z_m^n \ , \tag{13}$$

where $z_m \equiv \exp(-\mathrm{i}k'_m\tau)$ and $b_{\alpha m}$ are, generally complex, variational parameters. We assume that the number of frequencies in the signal is relatively small ($M \sim 50$ to 200). Although the system of nonlinear equations is, in general, still ill-conditioned, frequency filtering reduces the number of signal points, and hence the number of equations. In Ref. [11] three different methods, viz. linear predictor (LP), Padé approximant (PA), and signal diagonalization (SD) have been employed to solve Eq. (13) for a one-dimensional signal, i.e., $D = 1$. The SD method can be generalized in a straightforward manner to the harmonic inversion of cross-correlated periodic orbit sums. The problem of solving the nonlinear set of equations (13) can be recast in the form of the generalized eigenvalue problem [24, 25, 26]

$$\mathbf{U}\boldsymbol{B}_m = z_m \mathbf{S}\boldsymbol{B}_m \ , \tag{14}$$

where the elements of the $M \times M$ operator matrix $\mathbf{U}$ and overlap matrix $\mathbf{S}$ depend trivially upon the signal points:

$$\begin{aligned} U_{\alpha i,\alpha' j} &= c_{\alpha\alpha',i+j+1} \ ; \\ S_{\alpha i,\alpha' j} &= c_{\alpha\alpha',i+j} \ ; \quad i,j = 0,\ldots,N-1 \ . \end{aligned} \tag{15}$$

The matrices $\mathbf{U}$ and $\mathbf{S}$ in Eq. (14) are complex symmetric (i.e., non-Hermitian), and the eigenvectors $\boldsymbol{B}_m$ are orthogonal with respect to the overlap matrix $\mathbf{S}$,

$$(\boldsymbol{B}_m|\mathbf{S}|\boldsymbol{B}_{m'}) = N_m \delta_{mm'} \ , \tag{16}$$

where the brackets define a complex symmetric inner product $(a|b) = (b|a)$, i.e., no complex conjugation of either a or b. The overlap matrix $\mathbf{S}$ is not usually positive definite and therefore the N_m's are, in general complex, normalization parameters. An eigenvector $\boldsymbol{B}_m$ cannot be normalized for $N_m = 0$. The parameters $b_{\alpha m}$ in Eq. (13) are obtained from the eigenvectors $\boldsymbol{B}_m$ via

$$b_{\alpha m} = \frac{1}{\sqrt{N_m}} \sum_{\alpha'=1}^{D} \sum_{n=0}^{N-1} c_{\alpha\alpha',n} \boldsymbol{B}_{m,\alpha' n} \ . \tag{17}$$

The parameters z_m in Eq. (13) are given as the eigenvalues of the generalized eigenvalue problem (14), and are simply related to the frequencies k'_m in Eq. (12) via $z_m = \exp(-\mathrm{i}k'_m\tau)$.

The resolution of the results depends on the signal length. For a one-dimensional signal, the method requires a signal length of $s_{\max} \approx 4\pi\bar{\rho}(k)$, with $\bar{\rho}(k)$ the mean density of states, to resolve the frequencies [6]. This means that all periodic orbits up to the scaled action $s_{\max}$ have to be included. The advantage of using the cross-correlation approach is based on the insight that the total amount of independent information contained in the $D \times D$ signal is $D(D+1)$ multiplied by the length of the signal, while the total number of unknowns (here $b_{\alpha m}$ and k_m) is $(D+1)$ times the total number of poles k_m. Therefore the informational content of the $D \times D$ signal per unknown parameter is increased (compared to the one-dimensional signal) by roughly a factor of D, and the cross-correlation approach should lead to a significant improvement of the resolution. The power of this method for periodic orbit quantization has already been proven for the example of an integrable system [9, 10]. We will now demonstrate how the method works in the case of three touching disks, as an example of a chaotic system with extremely rapid proliferation of orbits and strong pruning.

B. Semiclassical eigenvalues of the closed three-disk system by harmonic inversion of a one-dimensional signal

We first investigate a one-dimensional signal ($N = 1$) by simply choosing $\hat{A}_1 = \mathbf{1}$, i.e., the unity operator. The signal is constructed from the set of periodic orbits shown in Fig. 4b, which contains about 5 million primitive orbits.

We analyzed the signal up to length $s_{\max} = 4.9$ using the decimated signal diagonalization method [11]. The frequencies obtained by harmonic inversion of the signal are the semiclassical approximations to the eigenvalues k_n. Fig. 6 shows the results from harmonic inversion (solid lines), compared with the exact quantum results (dashed lines), both presented in terms of the energy $E = (\mathrm{Re}\, k)^2/2$. The exact quantum eigenvalues were taken from Scherer [16] and Wirzba [27]. The harmonic inversion results clearly reproduce the quantum eigenvalues up to $E \approx 4500$ with only small deviations. However, the signal length was not sufficient to resolve the eigenvalues in the region $E > 4500$, where the density of states with respect to the wave number k (which grows $\sim \sqrt{E}$) becomes too large.

Apart from the values shown in Fig. 6, the harmonic inversion of the signal also yielded a number of unconverged frequencies. Converged frequencies were identified by having an imaginary part close to zero (since the eigenvalues of the wave number must be real for bound systems) and an amplitude close to the theoretical value $m_k = 1$. The whole set of frequencies obtained is shown in Figure 7 together with the real part of their amplitudes. The solid vertical lines mark the positions of the exact quantum eigenvalues. The semiclassical values in-

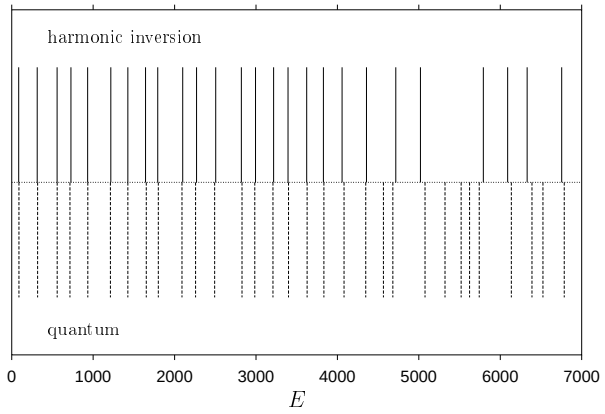

FIG. 6: Energy eigenvalues of the closed three-disk system (A_1 subspace). Dashed lines: exact quantum eigenvalues; solid lines: results $E = (\mathrm{Re}\, k)^2/2$ from harmonic inversion of a signal of length $s_{\max} = 4.9$.

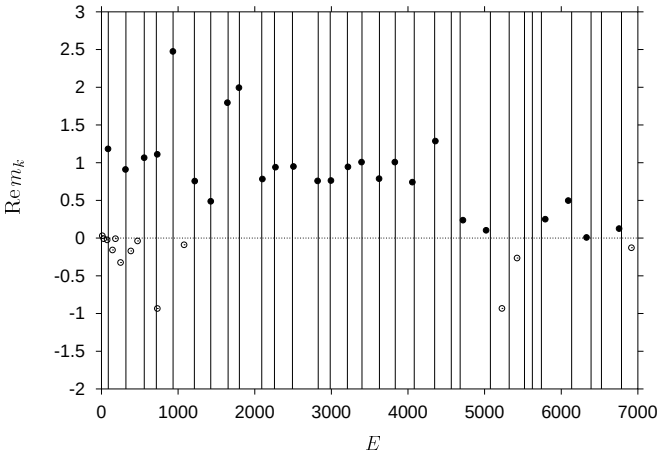

FIG. 7: Amplitudes of the whole set of values $E = (\mathrm{Re}\, k)^2/2$ (all circles) obtained for the energy eigenvalues of the closed three-disk system by harmonic inversion (including also unconverged values). The filled circles mark the values presented in Fig. 6. The solid vertical lines indicate the positions of the exact quantum eigenvalues.

cluded in Fig. 6 are represented by filled circles in Fig. 7. The amplitudes are not as well converged as the frequencies (i.e. the eigenvalues) but partly show larger deviations from the theoretical value $m_k = 1$. [This can be explained by the observation that when the decimated signal diagonalization method is used for harmonic inversion the frequencies usually converge faster than the amplitudes.] However, up to $E \approx 4500$, the eigenvalues can be clearly identified.

The small deviations of the eigenvalues obtained by harmonic inversion from the exact quantum values may have different reasons. Especially for the lowest eigenvalues, the major part is probably due to the semiclassical error. On the other hand, as explained above, we did not

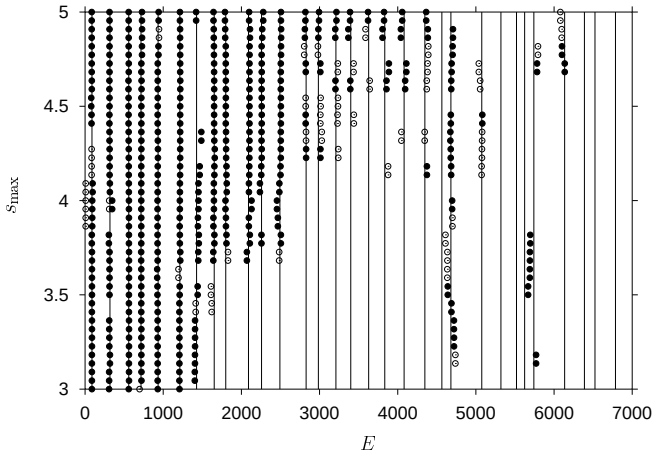

FIG. 8: Harmonic inversion results $E = (\mathrm{Re}\, k)^2/2$ for the energy eigenvalues of the closed three-disk system as a function of the signal length $s_{\max}$. Only results with $|\mathrm{Im}\, k| < 1.0$ and amplitudes $\mathrm{Re}\, m_k > 0.2$ are included. The filled circles mark values with $\mathrm{Re}\, m_k > 0.5$. (Solid vertical lines: positions of the exact quantum energies.)

include all orbits in the signal but left out a large number of relatively unstable orbits. Although each of these orbits only gives a negligible small contribution to the periodic orbit sum, the number of excluded orbits may be so large that their contributions sum up in a way so as to have a visible effect on the density of states. Finally, even in the low-lying part of the spectrum, deviations may arise from the fact that the signal length was very short. The influence of the missing orbits and the relatively short signal length are reflected in the relatively poor convergence of the amplitudes.

In order to test the stability of the results with respect to the signal parameters, and to obtain an estimate of random errors, we performed the same calculation with various sets of different signal parameters. Figure 8 shows the harmonic inversion results for the eigenvalues as a function of the signal length $s_{\max}$. From all frequencies obtained the values with $|\mathrm{Im}\, k| < 1.0$ and with amplitudes $\mathrm{Re}\, m_k > 0.2$ were singled out, respectively. The filled circles mark amplitudes with $\mathrm{Re}\, m_k > 0.5$. It can clearly be seen how the maximum eigenvalue up to which the spectrum can be resolved depends on the signal length. Fig. 8 shows that the results for the low-lying eigenvalues are quite stable with respect to variation of the signal length.

Compared with the results obtained by Tanner et al. [15] using the extended cycle expansion method, the analysis of a single signal by harmonic inversion has yielded about the same number of eigenvalues for the closed three-disk system. For the resolution of higher eigenvalues, the signal length was not sufficient. Extending the signal to significantly larger scaled actions is in practice not possible because of the extremely rapid increase of the number of orbits. It should be stressed,

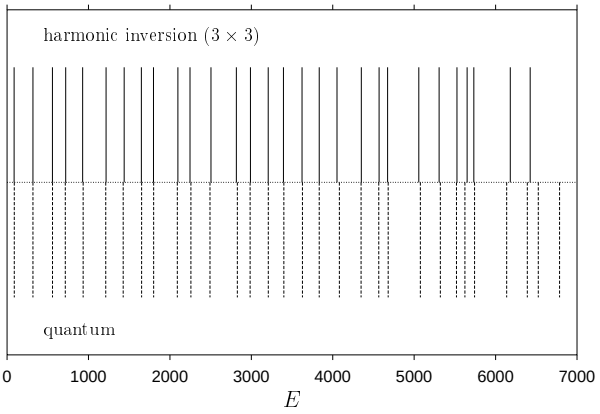

FIG. 9: Energy eigenvalues of the closed three-disk system (A_1 subspace). Dashed lines: exact quantum eigenvalues; solid lines: results $E = (\mathrm{Re}\, k)^2/2$ from harmonic inversion of a 3×3 cross-correlated signal with length $s_{\max} = 4.8$. The operators chosen for the construction of the signal are **1** (unity), r^4 and L^4, where r and L are the distance from the center of the system and the absolute value of the angular momentum, respectively.

however, that, in contrast to the cycle expansion method, which runs into severe problems because of the pruning of orbits in this system, it is at least *in principle* possible to improve the harmonic inversion results by including more orbits. On the other hand, as discussed before, the harmonic inversion method offers the possibility to significantly reduce the signal length required for the resolution of eigenvalues by the construction and analysis of cross-correlated periodic orbit sums.

C. Improvement of the resolution by harmonic inversion of cross-correlated periodic orbit sums

To increase the accuracy of the semiclassical eigenvalues, we now apply the cross-correlation technique to the closed three-disk system. Instead of the one-dimensional signal investigated in the previous section, we choose a set of three operators and construct a 3×3 cross-correlated signal according to Eq. (9). As input, we again use the set of periodic orbits presented in Fig. 4 together with the averages of different classical quantities over the orbits.

Fig. 9 shows the results from the harmonic inversion of a 3×3 signal of length $s_{\max} = 4.8$ (solid lines), which was constructed using the operators **1** (unity), r^4 and L^4, where r and L denote the distance from the center of the system and the absolute value of the angular momentum, respectively. The eigenvalues are again presented in terms of the energy $E = (\mathrm{Re}\, k)^2/2$. For comparison, the dashed lines indicate the positions of the exact quantum eigenvalues. The converged eigenvalues for the wave number k have been singled out from the whole set of frequencies obtained by the condition that they should have an imaginary part close to zero and an amplitude close

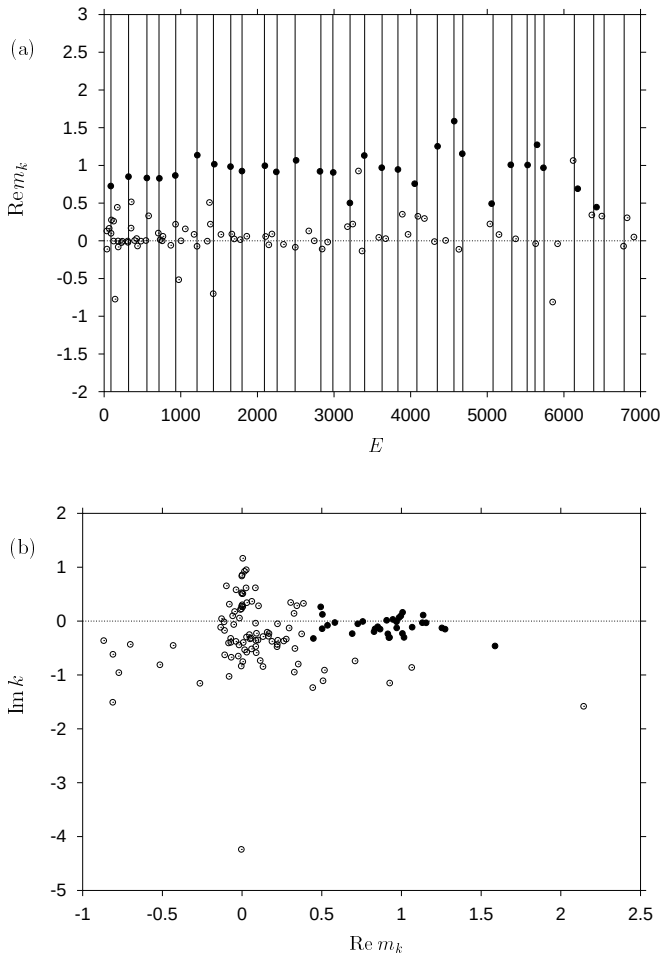

FIG. 10: Closed three-disk system: The whole set of frequencies (all circles) resulting from the analysis of the 3×3 signal (see Fig. 9). (a) Real part of the amplitudes versus energy $E = (\mathrm{Re}\, k)^2/2$. The solid vertical lines mark the positions of the exact quantum eigenvalues. (b) Imaginary part of the frequencies versus real part of the amplitudes. In both diagrams, the filled circles designate the values included in Fig. 9.

to the theoretical value $m_k = 1$. The amplitudes and the imaginary parts of all frequencies obtained are shown in Figure 10 by circles. In particular, the filled circles denote the frequencies included in Fig. 9. In Fig. 10a, the positions of the exact quantum eigenvalues are given by the solid vertical lines.

With the cross-correlated signal, one can now clearly identify eigenvalues up to $E \approx 6500$. In addition, the convergence of the lowest eigenvalues is improved as compared to the results from the single signal obtained in Section III B, as can be seen from the amplitudes. It is not possible to determine to what extent the accuracy of the semiclassical eigenvalues has improved since the results can only be compared with the exact quantum eigenvalues and the size of the semiclassical error is unknown.

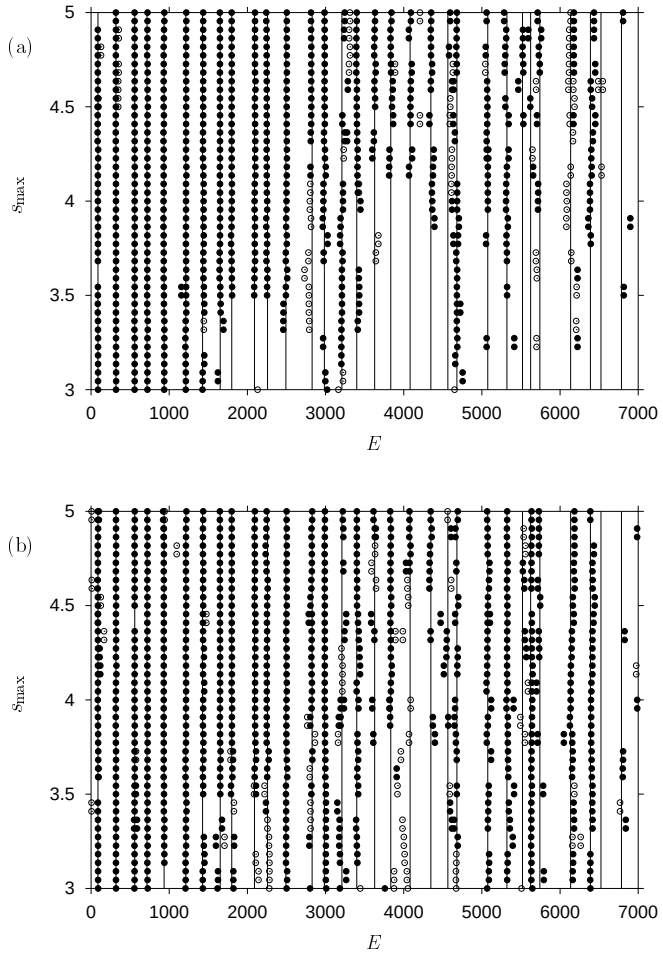

FIG. 11: Harmonic inversion results $E = (\mathrm{Re}\, k)^2/2$ for the energy eigenvalues of the closed three-disk system as a function of the signal length $s_{\max}$, calculated (a) from a 3×3 cross-correlated signal including the operators $\mathbf{1}$ (unity), r^4 and L^4 and (b) from a 4×4 signal including the operators $\mathbf{1}$, r^2, r^4 and L^4 (r: distance from the center of the system, L: absolute values of the angular momentum). Only results with $|\mathrm{Im}\, k| < 1.0$ and amplitudes $\mathrm{Re}\, m_k > 0.5$ are included. The filled circles mark values with $|\mathrm{Im}\, k| < 0.5$. The solid vertical lines indicate the positions of the exact quantum eigenvalues.

Again, we have performed the same calculation for various sets of parameters in the harmonic inversion scheme. Figure 11 shows the results from a 3×3 and from a 4×4 signal as functions of the signal length. The 3×3 signal was constructed from the operators $\mathbf{1}$ (unity), r^4 and L^4, and the 4×4 signal contained the operators $\mathbf{1}$, r^2, r^4 and L^4. In both diagrams, only the frequencies with an imaginary part $|\mathrm{Im}\, k| < 1.0$ and an amplitude $\mathrm{Re}\, m_k > 0.5$ were included. The filled circles mark values with $|\mathrm{Im}\, k| < 0.5$. The positions of the exact quantum eigenvalues are again marked by the solid vertical lines.

As with the one-dimensional signal analyzed in the previous section, it can be observed that the results for the lowest eigenvalues are very stable with respect to the variation of the signal length as long as the signal is not too short. However, the very lowest frequencies show a tendency to split into two or more, which was a frequent observation in our calculations when the signal length and the matrix dimensions were chosen too large. The results for the higher eigenvalues depend more sensitively on the signal length as the density of states approaches the limiting resolution that can be achieved with the signal. In this region, the 4×4 signal shows a better resolution than the 3×3 signal.

With the 3×3 signal and the two largest values of the signal length considered, the lowest eigenvalue was not obtained. The reason for this probably lies in inaccuracies at the end of the signal, as the signal length approaches the value $s_{\max} = 5.0$: In the decimated signal diagonalization scheme, which we used for the harmonic inversion of the signal, the δ functions in the original signal (9) are replaced with sinc functions [11] [$\mathrm{sinc}\, x = (\sin x)/x$]. Therefore, every periodic orbit contributes to the signal not only exactly at its scaled action $s = s_{\mathrm{po}}$, but also in a range Δs around this point. If the signal length is close to $s_{\max} = 5.0$, also orbits with actions slightly larger than this limit may give non-negligible contributions to the very end of the signal. Since we did only include orbits with $s \leq 5.0$, these contributions are missing in our signal.

Some eigenvalues between $E = 3500$ and $E = 5000$ seem to be particularly hard to obtain from the set of orbits used. Possibly, these eigenvalues are related to the orbits running very deep into the corners between the disks, which were not included in the signal. We conjecture that the missing orbits as well as the short signal length are again responsible for the deviations especially of the results for higher eigenvalues from the exact quantum values.

IV. CONCLUSION

We have successfully applied the technique of harmonic inversion to the semiclassical quantization of a system with an extremely rapid proliferation of periodic orbits and strong pruning. With the harmonic inversion of cross-correlated periodic orbit sums we were able to calculate accurate semiclassical energy eigenvalues of the closed three-disk system up to the region $E \approx 6500$ (a total of 29 levels). This is the first time that such high-lying eigenvalues have been correctly calculated by periodic orbit theory in this system. Our results demonstrate that the harmonic inversion of cross-correlated periodic orbit sums is indeed a powerful method of periodic orbit quantization and allows the stable handling even of huge periodic orbit sets. In contrast to other methods, which depend on the existence of a complete symbolic code, the harmonic inversion technique is not affected by the strong pruning of orbits. In the closed three-disk system, the only restriction for the practical application of the harmonic inversion method lies in the extremely

large number of periodic orbits, which is a special feature of this system. It should also be noted that the semiclassical eigenvalues were obtained without resorting to the mean density of states, which, including all necessary correction terms, is nontrivial to calculate even in the case of the closed three-disk system [16]. The present results may stimulate future work on other challenging systems without special structural information on the quantum or classical level. One example with strong pruning of the symbolic dynamics is the three-dimensional generalization of the closed three-disk billiard, i.e., a system consisting of four touching spheres at the corners of a regular tetrahedron. By contrast to the closed three-disk system this is an open system where no functional equation can be applied. Experiments on chaotic light-scattering from the four spheres have recently attracted much attention [28].

Acknowledgments

We thank A. Wirzba for communicating to us quantum mechanical data for the closed three-disk system. This work was supported by Deutsche Forschungsgemeinschaft and Deutscher Akademischer Austauschdienst.

[1] M. C. Gutzwiller, *Chaos in Classical and Quantum Mechanics*, Springer, New York, 1990.
[2] A. Inomata et al. (eds.), *Festschrift in honor of Martin Gutzwiller*, Foundations in Physics **31**, 2001.
[3] P. Cvitanović and B. Eckhardt, Phys. Rev. Lett. **63**, 823 (1989).
[4] R. Aurich, C. Matthies, M. Sieber, and F. Steiner, Phys. Rev. Lett. **68**, 1629 (1992).
[5] M. V. Berry and J. P. Keating, J. Phys. A **23**, 4839 (1990).
[6] J. Main, V. A. Mandelshtam, and H. S. Taylor, Phys. Rev. Lett. **79**, 825 (1997).
[7] J. Main, V. A. Mandelshtam, G. Wunner, and H. S. Taylor, Nonlinearity **11**, 1015 (1998).
[8] J. Main, Phys. Rep. **316**, 233 (1999).
[9] J. Main, K. Weibert, V. A. Mandelshtam, and G. Wunner, Phys. Rev. E **60**, 1639 (1999).
[10] K. Weibert, J. Main, and G. Wunner, Eur. Phys. J. D **12**, 381 (2000).
[11] J. Main, P. A. Dando, D. Belkić, and H. S. Taylor, J. Phys. A **33**, 1247 (2000).
[12] B. Eckhardt and G. Russberg, Phys. Rev. E **47**, 1578 (1993).
[13] B. Eckhardt, G. Russberg, P. Cvitanović, P. E. Rosenqvist, and P. Scherer, in *Quantum Chaos*, edited by G. Casati and B. V. Chirikov, page 405, Cambridge University Press, Cambridge, 1995.
[14] A. Wirzba, Phys. Rep. **309**, 1 (1999).
[15] G. Tanner, P. Scherer, E. B. Bogomolny, B. Eckhardt, and D. Wintgen, Phys. Rev. Lett. **67**, 2410 (1991).
[16] P. Scherer, PhD thesis, Universität Köln, 1991.
[17] P. Gaspard and S. A. Rice, J. Chem. Phys. **90**, 2225, 2242, 2255 (1989).
[18] K. T. Hansen, Nonlinearity **6**, 753 (1993).
[19] P. Cvitanović and B. Eckhardt, Nonlinearity **6**, 277 (1993).
[20] E. B. Bogomolny, Physica D **31**, 169 (1988).
[21] J. Main and G. Wunner, Phys. Rev. E **60**, 1630 (1999).
[22] S. Hortikar and M. Srednicki, Phys. Rev. E **61**, R2180 (2000).
[23] E. Narevicius, D. Neuhauser, H. J. Korsch, and N. Moiseyev, Chem. Phys. Lett. **276**, 250 (1997).
[24] V. A. Mandelshtam, J. Chem. Phys. **108**, 9999 (1998).
[25] M. R. Wall and D. Neuhauser, J. Chem. Phys. **102**, 8011 (1995).
[26] V. A. Mandelshtam and H. S. Taylor, J. Chem. Phys. **107**, 6756 (1997); **109**, 4128 (1998) (erratum).
[27] A. Wirzba, private communication.
[28] D. Sweet, E. Ott, and J. A. Yorke, Nature **399**, 315 (1999).